

Award Accounts

The Chemical Society of Japan Award for Creative Work for 2005

Rational Syntheses of Multinuclear High-Spin Complexes

Hiroki Oshio* and Masayuki Nihei

Graduate School of Pure and Applied Sciences, Department of Chemistry, University of Tsukuba,
1-1-1 Tennodai, Tsukuba 305-8571

Received May 9, 2006; E-mail: oshio@chem.tsukuba.ac.jp

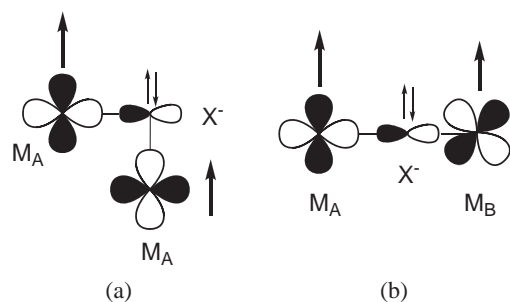
Magnetic interactions within or between molecules are typically antiferromagnetic, and careful design of multinuclear complexes by considering magnetic orbital symmetry and bridging structures is necessary for preparing metal complexes with high-spin ground states. First, we present the rational syntheses of high-spin molecules with ferromagnetic interactions. In the latter part of this article, our synthetic methodology for high-spin molecules was applied to prepare homo- and hetero-metal single-molecule magnets (SMMs). In the homo-metal SMMs, high-spin ground states can be achieved by assembling ferrous ions in the cubic shape, and they show superparamagnetic behavior due to easy axis magnetic anisotropy of the molecules. Furthermore, control of magnetic anisotropy of single ions and multinuclear complex molecules is presented. A facile one-pot synthesis for hetero-metal complex has been developed, and SMM behaviors of the obtained hetero-metal clusters are presented.

Magnetic interactions within or between molecules are typically antiferromagnetic, which is in accord with molecular orbital considerations. When two magnetic orbitals, each having an electron, interact, they form antibonding and bonding orbitals. In the antiferromagnetic interactions, the two electrons locate in the bonding orbital with anti-parallel spin alignment, and this situation can be regarded as a very weak chemical bond. The magnetic interaction (J) can be expressed as the sum of exchange integral (K) and $2\beta S$ (β = transfer integral and S = overlap integral), which favor ferromagnetic and antiferromagnetic interactions, respectively. It should be pointed that, for the occurrence of ferromagnetic interactions, metal ions have no orbital overlap but have exchange interactions. In order to bring about ferromagnetic interactions, the following situations are needed.¹ (i) When magnetic orbitals are strictly or accidentally orthogonal to each other, the magnetic interaction becomes ferromagnetic.² Magnetic orbitals of π - and σ -spins are strictly orthogonal each other, while right-angled arrangements of homo-magnetic orbitals give no orbital overlaps, and this situation is called accidental orthogonality. (ii) Configuration interactions of a ground high-spin with excited high-spin states stabilize the high-spin ground state.³ (iii) Topological symmetry of π -electron network must be considered to design high-spin organic molecules, such as poly-carbenes.⁴ Spin polarization, a strategy originally suggested by McConnell,⁵ can lead to ferromagnetic interactions and can be applied to metal complexes.⁶ It is pointed out that direct or indirect charge-transfer (CT) interactions between the paramagnetic centers enhance magnetic interactions, and such effects are treated with a valence bond-like approach.

In designing high-spin molecules, careful considerations

about the symmetry of the magnetic orbitals and bridging structures should be devoted. High-spin ground states can be achieved by ferromagnetic interactions between metal ions or by ferrimagnetic interactions between metal ions with different spin multiplicities. Homo-metal systems require ferromagnetic interactions to have high-spin ground states, while in hetero-metal systems both ferro- and ferrimagnetic situations can be used to have high-spin ground states. Magnetic interactions between metal centers are governed by many factors. However, a superexchange mechanism is often predominant involving magnetic interactions, and the sign of the exchange coupling constants can be predicted by bridging structures. When two homo-metal ions are bridged by a single anion with a bridging angle of 180° , for example, strong antiferromagnetic interactions ($J < 0$) occur via ligand-to-metal (LM) CT interactions, and a low-spin ground state is stabilized. When homo-metal ions are linked without magnetic orbital overlap, two metal ions bridged with a bond angle of 90° , ferromagnetic interactions occur, stabilizing a high-spin ground state (Scheme 1a). In the case of hetero-metal systems, each having orthogonal magnetic orbitals, the metal ions that are bridged with a bond angle of 180° would lead to ferromagnetic coupling (Scheme 1b).

First, we describe rational syntheses of high-spin molecules, molecules with high-spin ground state, by the ferromagnetic interactions. During the course of extending our research to high-spin molecules, a dodecanuclear manganese complex, $[\text{Mn}_{12}\text{O}_{12}(\text{O}_2\text{CMe})_{16}(\text{H}_2\text{O})_4]$ ([Mn12]),⁷ has been proven to show superparamagnetism at very low temperature and named a single-molecule magnet (SMM). High-spin molecules with easy-axis magnetic anisotropy show slow magnetic relaxation



Scheme 1. Ferromagnetic interactions in (a) homo-metal and (b) hetero-metal systems.

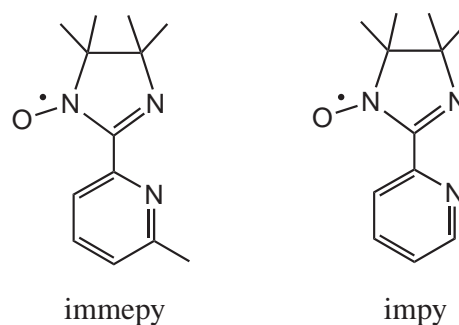


Chart 1.

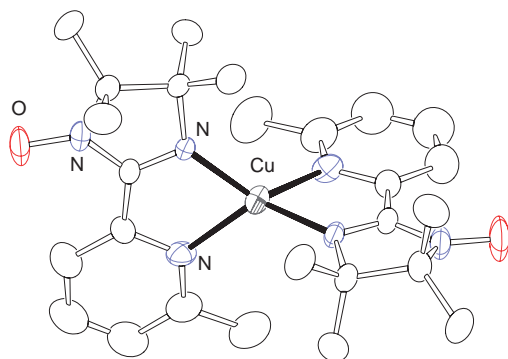
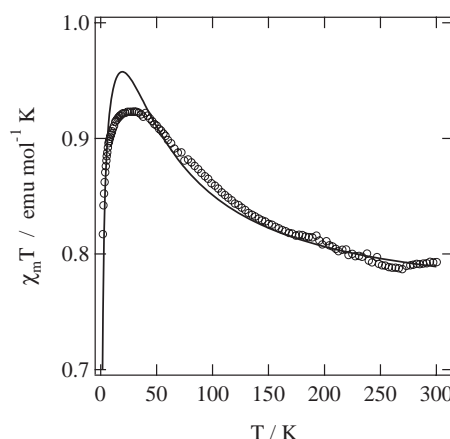


Fig. 1. Structure and magnetic susceptibility data of $[\text{Cu}^{\text{I}}(\text{immepy})_2]^+$.



of the spin reorientation along the magnetic anisotropy axis, and at very low temperature, the spin does not thermally flip but flips via quantum processes. These molecules have a double minimum potential for the reversal of the magnetic moment.⁸ One feature of SMMs is a hysteresis effect in the magnetization process originating from the slow magnetic relaxation, which make it possible to store information in a single molecule.⁹ The second fascinating feature of SMMs is that the relaxation of the magnetization shows clear quantum effects, and accordingly, SMMs can be used to investigate the mesoscopic range in which quantum and classical behavior coexist. We applied our synthetic methods for preparing high-spin molecules to the synthesis of homo- and hetero-metal SMMs.

High-Spin Molecules with Ferromagnetic Interactions

Orthogonal Arrangement of Magnetic Orbitals: d^{10} Metal Complexes with Imino Nitroxide.¹⁰ Magnetic interactions between paramagnetic centers through diamagnetic metal ions have been considered to be negligibly small or weakly antiferromagnetic. However, metal complexes of diamagnetic metal ions with semiquinones show a variety of magnetic interactions depending on metal ions and coordination geometries. A series of square-planar metal complexes $[\text{M}^{\text{II}}(\text{sq})_2]$ ($\text{M} = \text{Ni}$, Pd , and Pt ; $\text{sq} = \text{tert-butyl-substituted semiquinone}$) shows fairly strong antiferromagnetic interactions due to indirect overlap of the magnetic orbitals through the metal $d\pi$ orbitals.¹¹ The strength of inter-radical exchange increases down the series of metal ions, i.e., the strongest cou-

pling for Pt and the weakest for Ni . Pseudo-octahedral coordination geometry provides for orthogonal coordination of semiquinones. $[\text{M}^{\text{III}}(3,6\text{-dbsq})_3]$ ($\text{M} = \text{Al}$ and Ga)¹² and $[\text{Ga}^{\text{III}}(3,5\text{-dbsq})_3]$ ¹³ (Ligands: semiquinone derivatives) showed weak ferromagnetic interactions ($J = 6.2$, 8.6 , and 7.8 cm^{-1} with $H = -2J\Sigma S_i \cdot S_j$), while $[\text{M}^{\text{IV}}(\text{cat-N-sq})_2]$ ($\text{M} = \text{Ti}$, Ge , and Sn) (Cat-N-SQ = tridentate Schiff base biquinone)¹⁴ were characterized by a triplet ground state with $J = -56$, -27 , and -23 cm^{-1} ($H = J\Sigma S_1 \cdot S_2$), respectively. It should be noted that magnitude of magnetic interactions through diamagnetic ions depends strongly on energy level of the $d\pi$ orbitals and that the charge-transfer interactions determine the sign and amplitude of magnetic interactions. In this section, ferromagnetic interactions of two coordinating iminonitroxide derivatives (immepy and impy) with d^{10} metal ions are presented, and the role of CT interactions is discussed (Chart 1).

Cu^+ ions favor a tetrahedral coordination geometry,¹⁵ which is suitable for the orthogonal arrangement of two bidentate ligands. The geometry causes an orthogonal arrangement to the two coordinating bidentate radical ligands, leading to ferromagnetic interaction between the radicals. The complex $[\text{Cu}^{\text{I}}(\text{immepy})_2](\text{PF}_6)$, where immepy is a bidentate imino nitroxide, 2-[2-(6-methylpyridyl)]-4,4,5,5-tetramethyl-4,5-dihydro-1H-imidazolyl-1-oxyl, has a C_2 axis, and the Cu^+ ion is coordinated by crystallographically equivalent immepy ligands acting as bidentate ligands (Fig. 1). The coordination geometry about Cu^+ ion is pseudotetrahedral with the four coordination sites being occupied by four nitrogen atoms, and the two radical planes (magnetic orbitals) are perpendicular to each other

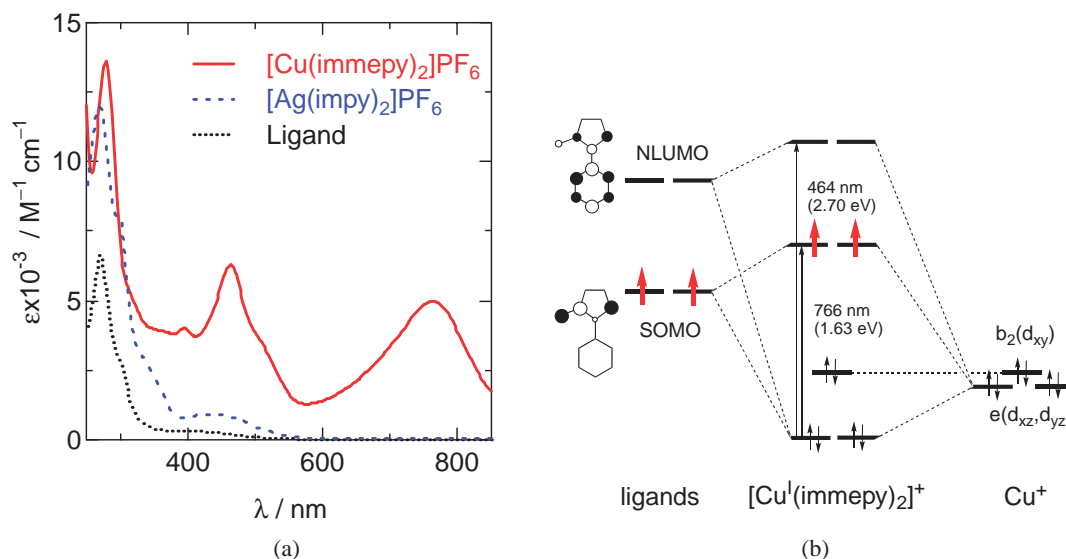


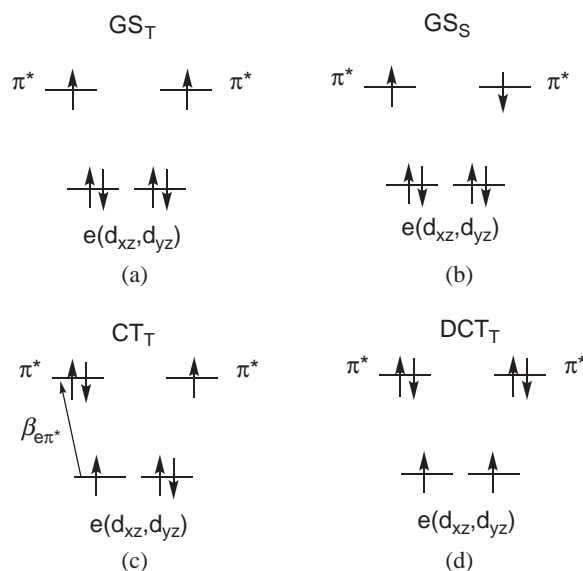
Fig. 2. (a) Absorption spectra of Cu^+ and Ag^+ imino nitroxides, and (b) the MO scheme and band assignments of Cu^+ complex under the pseudotetrahedral coordination geometry.

with the dihedral angle of 88.7° . Magnetic susceptibility measurements showed that the coordinated iminonitroxides are ferromagnetically coupled and J was estimated to $55.1(2)\text{cm}^{-1}$ using a fixed g value of 2.0 and $H = -J\sum S_1 \cdot S_2$. It is noted that $[\text{Cu}^{\text{I}}(\text{impepy})_2](\text{PF}_6)$ in acetonitrile showed intense absorption bands at 766 nm ($\epsilon = 5000\text{M}^{-1}\text{cm}^{-1}$) and 464 nm ($\epsilon = 6300\text{M}^{-1}\text{cm}^{-1}$) with a shoulder band at 514 nm (Fig. 2a). These bands were assigned by comparison to the electronic spectra of Cu^+ -diimine¹⁶ and Cu^+ -semiquinone complexes.¹⁷ The intense band at 464 nm and shoulder at 514 nm were assigned to MLCT bands, $e(d_{xz}, d_{yz}) \rightarrow e(\pi^*)$ (NLUMO) and $b_2(d_{xy}) \rightarrow e(\pi^*)$ transitions, respectively, and the lower energy band (766 nm) corresponds to a $e(d_{xz}, d_{yz}) \rightarrow \text{SOMO}$ (impepy) transition (Fig. 2b).

The mechanism, which determines the relative energy (J) of the triplet and singlet states, has been often discussed in terms of the Heitler–London interaction and valence bond configuration interaction between the ground and CT states.¹⁸ J depends primarily on the Heitler–London type interaction within the ground state and in natural magnetic orbital treatments the triplet–singlet energy gap is expressed as:

$$J_{\text{GS}} = 2K_{\pi^*\pi^*} + 4\beta_{\pi^*\pi^*}S_{\pi^*\pi^*} \quad (1)$$

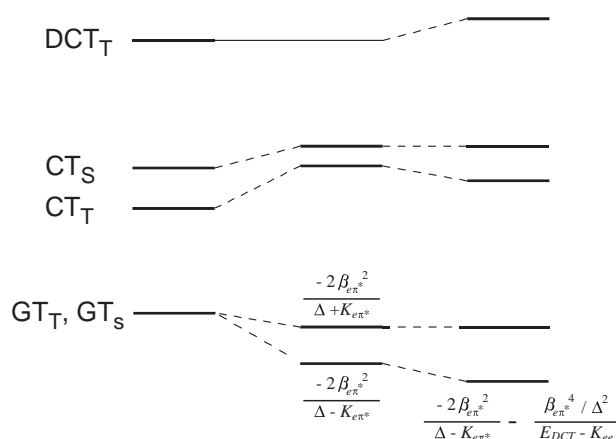
$2K_{\pi^*\pi^*}$, $\beta_{\pi^*\pi^*}$, and $S_{\pi^*\pi^*}$ represent the two electron exchange, transfer, and overlap integrals between radical SOMOs, respectively. The two coordinating radicals are orthogonally arranged, $S_{\pi^*\pi^*}$ becomes zero, and strong ferromagnetic coupling primarily arises from $2K_{\pi^*\pi^*}$. $[\text{Cu}^{\text{I}}(\text{impepy})_2](\text{PF}_6)$ has a fairly strong CT band, which is due to the π -back donation to the radical SOMO. It is necessary to consider valence bond configuration interactions to interpret the ferromagnetic interaction. Valence bond-like treatments have been invoked to explain ferromagnetic interactions or ordering in metal complexes as well as in pure organic compounds. For example, Goodenough proposed that interactions between half-filled orbitals on one metal and empty orbitals on the other metal can contribute to ferromagnetic interactions.¹⁹ This mechanism was also invoked to justify the ferromagnetic ordering



Scheme 2. (a) Ground triplet and (b) ground singlet states configurations, and (c) one and (d) two electrons charge-transfer configurations.

observed for (*p*-nitrophenyl)nitronyl nitroxide,²⁰ and ferromagnetic interactions in $[\text{Mn}^{\text{III}}(\mu\text{-O})(\mu\text{-CH}_3\text{CO}_2)_2\text{Mn}^{\text{III}}]$ ²¹ and $[\text{Gd}_2\text{Cu}_4]$.²² The situation is not the same as the above case but is closer to the models by McConnell and Breslow.²³ The coordination geometry (D_{2d}) about the Cu^+ ion is assumed to be pseudotetrahedral, and the orthogonal orbitals were used in the following treatment. Based on the four-orbitals (degenerate $e(d_{xz}, d_{yz})$ and degenerate π^* orbitals) and six-electrons (four on $e(d_{xz}, d_{yz})$ and two on each π^*), the ground triplet (GS_T) and singlet (GS_S) configurations are represented by Schemes 2a and 2b.

The MLCT configuration generated by the CT transition from e to π^* is represented by Scheme 2c, where $\beta_{e\pi^*}$ is a transfer integral. This MLCT state has both triplet (CT_T) and singlet (CT_S) configurations. However, the triplet is lower in



Scheme 3.

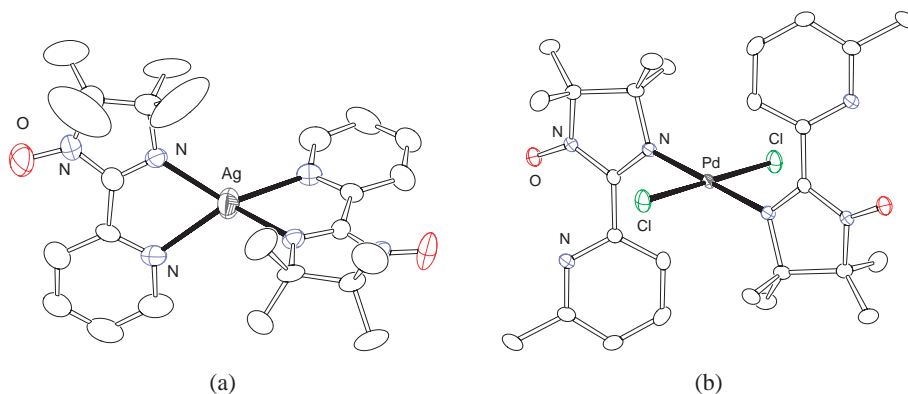
energy than the singlet due to the orthogonality of the singly occupied e and π^* orbitals (Scheme 3). The ground and MLCT states are mutually repulsive, and the admixed triplet and singlet ground states are stabilized by $-2\beta_{e\pi^*}^2/(\Delta - K_{e\pi^*})$ and $-2\beta_{e\pi^*}^2/(\Delta + K_{e\pi^*})$, respectively, where Δ is the cost in energy of transferring an electron from e to π^* and $K_{e\pi^*}$ is the interatomic exchange integral involving the orbitals e and π^* . As a consequence of mixing, the ground triplet state is lower than the singlet and the triplet–singlet energy gap (J) is expressed as $J = 4K_{e\pi^*}\beta_{e\pi^*}^2/(\Delta^2 - K_{e\pi^*}^2)$ (Scheme 3). There is the more excited CT configuration. Starting from the MLCT configuration (Scheme 2c), an electron on a doubly occupied e orbital can be transferred to a singly occupied π^* orbital such that the Cu^+ ion possesses two singly occupied orbitals (Scheme 2d). By comparison with the GS configuration (Scheme 2a), this corresponds to a double CT configuration (DCT_T), and this configuration should be a triplet due to the Hund's rule. The interaction between the GS_T and DCT_T configurations stabilizes the GS_T triplet, because the singlet DCT_S configuration is quite high in energy. The resulting stabilization of the GS_T is $-(\beta_{e\pi^*}^4/\Delta^2)/(E_{\text{DCT}} - K_{ee})$, where E_{DCT} and K_{ee} correspond to the energy cost associated with this electron transfer and the one-site exchange integral, respectively. Stabilization due to the DCT is, in general, very small. In this case, however, the two unpaired electrons locate on the Cu ion in the DCT configuration, which leads to the fairly large K_{ee} . Hence, the GS_T – DCT_T configuration interaction can not be ig-

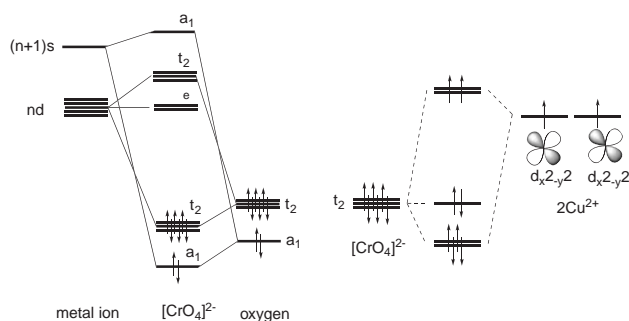
nored. As the result of the configuration interaction of the GS_T with CT_T and DCT_T , the GS_T is stabilized by $-2\beta_{e\pi^*}^2/(\Delta - K_{e\pi^*}) - (\beta_{e\pi^*}^4/\Delta^2)/(E_{\text{DCT}} - K_{ee})$ (Scheme 3).²⁴

Magnetic interactions in $[\text{Ag}^{\text{I}}(\text{impy})_2](\text{PF}_6)$ were also examined (Fig. 3a). The coordination geometry about the Ag^+ ion deviates from tetrahedral with a dihedral angle of the coordinating imino nitroxides of 79.2° , which results in the broken orthogonality of the coordinating imino nitroxides. Powder magnetic susceptibility and EPR spectrum of frozen acetonitrile solution suggested that the magnetic interaction between the coordinating imino nitroxide is weakly ferromagnetic. It should be noted that $[\text{Ag}^{\text{I}}(\text{impy})_2](\text{PF}_6)$ did not show MLCT bands (Fig. 2a), which confirms an apparent energy mismatch between the ligand π^* and $d\pi$ orbital of the Ag^+ ion. It can be concluded that not only the broken orthogonality but also the lack of the MLCT interaction make the intramolecular ferromagnetic interaction very weak in the case of $[\text{Ag}^{\text{I}}(\text{impy})_2](\text{PF}_6)$. It is also pointed out that square-planar complex of $[\text{Pd}^{\text{II}}\text{Cl}_2(\text{impepy})_2]$ showed a fairly strong antiferromagnetic interaction ($J = -160.8 \text{ cm}^{-1}$) between coordinating two imino nitroxides (Fig. 3b).²⁵ $[\text{Pd}^{\text{II}}\text{Cl}_2(\text{impepy})_2]$ showed strong absorption bands at 350 nm ($7800 \text{ dm}^3 \text{ mol}^{-1} \text{ cm}^{-1}$) and 500 nm ($1800 \text{ dm}^3 \text{ mol}^{-1} \text{ cm}^{-1}$), assigned to be metal to NLUMO and the metal to SOMO transitions. This confirms that the metal d_{xy} orbital has substantial overlap with the SOMOs and leads to the strong antiferromagnetic interaction.

Chromate Bridges.²⁶ Bridging ligands usually mediate antiferromagnetic interactions due to the magnetic orbital overlap through bridges. Ferromagnetic interactions, however, can occur, when the magnetic orbitals are (accidentally) orthogonal to each other. In this section, magnetic interactions through tetraoxometalates will be discussed by means of frontier orbital symmetry.

Oxometalate anions like $[\text{CrO}_4]^{2-}$ have tetrahedral coordination geometry, and d -orbitals split into e and t_2 type orbitals under the T_d symmetry (Scheme 4). The e pair of the d -orbitals has no matching combination of the oxygen orbitals and remains nonbonding. The three t_2 orbitals, however, have the same symmetry with combinations of coordinating oxygen orbitals, and form bonding and antibonding orbitals. The t_2 -type bonding orbitals, which mainly consist of the oxygen orbitals, are occupied by six electrons from the oxygen atoms. When two paramagnetic metal ions having d_σ spins like Cu^{2+} ions are bridged by the $[\text{CrO}_4]^{2-}$ unit, two of the t_2 -type orbitals

Fig. 3. Structures of (a) $[\text{Ag}(\text{impy})_2]^+$ and (b) $[\text{Pd}^{\text{II}}\text{Cl}_2(\text{impepy})_2]$.



Scheme 4. Orbital schemes of $[\text{CrO}_4]^{2-}$ and its dicopper complex.

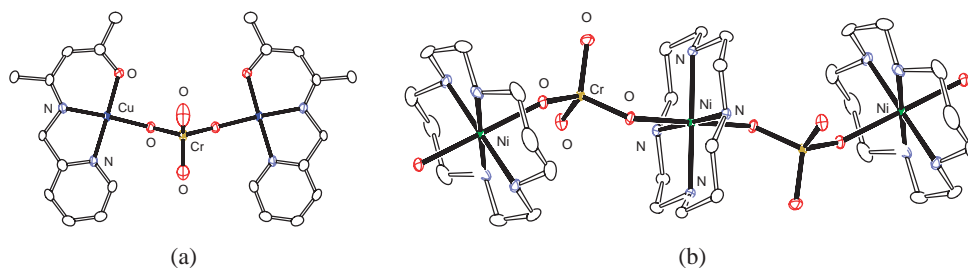


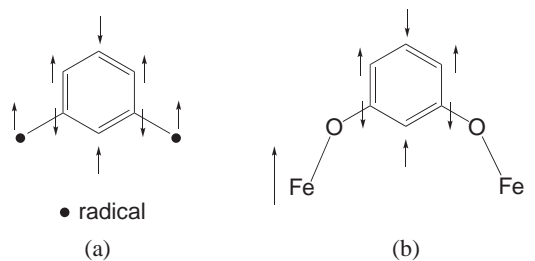
Fig. 4. Structures of $[\text{CrO}_4]^{2-}$ bridged (a) dinuclear Cu^{2+} and (b) one-dimensional Ni^{2+} complexes.

and σ -type ($d_{x^2-y^2}$) magnetic orbitals of the Cu^{2+} ions form bonding and antibonding orbitals (Scheme 4). The two unpaired electrons from Cu^{2+} ions locate on doubly degenerate antibonding orbitals, leading to ferromagnetic interactions.

A chromato-bridged dicopper(II) complex of $[\{\text{Cu}^{\text{II}}(\text{acpa})\}_2(\mu\text{-CrO}_4)] \cdot 4\text{CH}_3\text{OH} \cdot 4\text{H}_2\text{O}$ ($\text{Hacpa} = N$ -(1-acetyl-2-propylpyridene)(2-pyridylmethyl)amine) showed ferromagnetic behavior with $J = +7.3(1)\text{cm}^{-1}$ and $g = 2.12(1)$ (Fig. 4a). The chromato-bridged dicopper complex has only mirror symmetry; hence, the molecular geometry of the complex is C_s . In spite of the fact that there are no degenerate orbitals under C_s symmetry, the antibonding orbitals that form should have a very small energy gap or be accidentally degenerate due to the rigid structure of the $[\text{CrO}_4]^{2-}$ unit. Therefore, two unpaired electrons from the two paramagnetic centers locate on the accidentally degenerate antibonding orbitals, and this leads to ferromagnetic interaction between the bridged Cu^{2+} centers. It should be noted that $[\text{CrO}_4]^{2-}$ bridges $[\text{Ni}(\text{cyclam})]^{2+}$ and forms a ferromagnetic chain, *catena*-poly $[\text{Ni}(\text{cyclam})(\mu\text{-CrO}_4\text{-}O,O') \cdot 2\text{H}_2\text{O}]$, with $J = +0.6(1)\text{cm}^{-1}$ and $g = 2.13(1)$ (Fig. 4b).²⁷

Topological Approach. Some strategies for incorporating ferromagnetic interactions into organic multi-radical compounds have been proposed.²⁸ A spin polarization mechanism, i.e., topological symmetry of the π electron network, was applied to design high-spin organic molecules in poly-carbene system. Some poly-carbenes, in which the carbenes are linked in meta-positions of a benzene-ring, have shown fairly strong ferromagnetic interaction, and the ferromagnetic interaction between radicals can be explained by polarized $p\pi$ spin over the whole molecule which forms a topological network (Scheme 5).

Is it possible to apply the spin polarization mechanism to designing multi-nuclear complexes with an intramolecular fer-



Scheme 5. π spin topology in (a) dicarbene and (b) resorcinol-bridged Fe^{3+} complex.

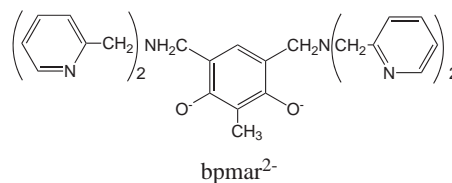


Chart 2.

romagnetic interaction? Yes, paramagnetic metal ions that are linked with an aromatic bridging ligands in the meta-position have ferromagnetic interactions due to the topologically networked $d\pi$ spins to the ligand $p\pi$ orbitals. The ligand 4,6-bis $[N,N$ -bis(2-pyridylmethyl)aminomethyl]-2-methylresorcinol (H_2bpmar) was used to bridge Fe^{3+} ions. A dinuclear Fe^{3+} complex, $[\text{Fe}^{\text{III}}_2(\text{bpmar})(\text{H}_2\text{O})_4](\text{NO}_3)_4 \cdot 3\text{H}_2\text{O}$, fulfills conditions required for the occurrence of ferromagnetic interactions.²⁹ (i) Central metal ions have $d\pi$ spins. (ii) Organic bridging ligands should have de-stabilized HOMOs, which are close in energy to the magnetic orbitals of the metal ions. (iii) A topological network concerning the $d\pi$ spin to the ligand $p\pi$ orbitals must exist (Chart 2).

Magnetic susceptibility measurements of $[\text{Fe}_2(\text{bpmar})(\text{H}_2\text{O})_4](\text{NO}_3)_4 \cdot 3\text{H}_2\text{O}$ showed ferromagnetic behavior, and J was estimated to be $+0.65(3)\text{cm}^{-1}$ with $g = 1.953(4)$ by using the data above 10 K (Fig. 5). It is apparent that the metal ion should have $d\pi$ spin in order to interact or mix with the organic $p\pi$ orbital. Simple perturbation theory predicts that two orbitals can strongly interact when the orbitals have the same symmetry and comparable energies, and a metal ion must have a magnetic $d\pi$ orbital, of which energy is close to that of $p\pi$ orbital of organic bridges. Resorcinol has a de-stabilized HOMO (highest occupied molecular orbital) due to the two negative charges; hence, $d\pi$ orbitals of an Fe^{3+} ion become closer in energy to the $p\pi$ orbitals of the resorcinol. The spin

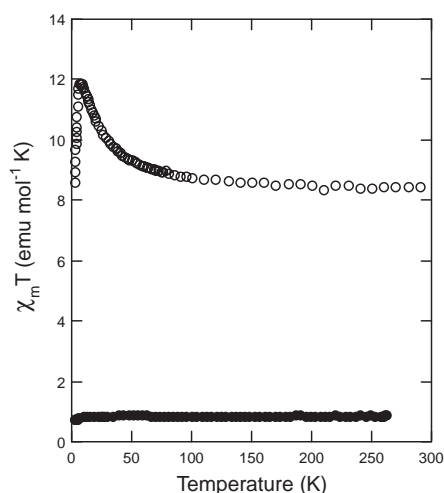


Fig. 5. Magnetic data of (○) $[\text{Fe}_2(\text{bpmar})(\text{H}_2\text{O})_4](\text{NO}_3)_4 \cdot 3\text{H}_2\text{O}$ and (●) $[\text{Cu}_2(\text{bpmar})(\text{NCS})_2] \cdot 4\text{H}_2\text{O}$.

polarization of the $d\pi$ spins to the bridging ligands occurs to give ferromagnetic interaction (Scheme 5b). It is also pointed out that the dinuclear Cu^{2+} complex $[\text{Cu}_2(\text{bpmar})(\text{NCS})_2] \cdot 4\text{H}_2\text{O}$ did not show any ferromagnetic interactions (Fig. 5), which confirms that $d\pi$ spin topology plays an important role leading to ferromagnetic interactions.²⁷

Single Molecule Magnets

High-spin molecules with magnetic anisotropy have been proven to exhibit non-classical magnetic properties. High-spin molecules with an easy axis type of anisotropy have a double minimum potential in the reversal of the magnetic moment (Fig. 6a), and they show slow magnetic relaxation owing to a energy barrier in respect to spin flipping along the magnetic anisotropy axis. At very low temperatures, the spin does not flip thermally, but flips via quantum processes. Thus, the high-spin molecules behave as if they are molecular-size permanent magnets. Molecules having this superparamagnetic behavior are called single-molecule magnets (SMMs).³⁰ One of the features of SMMs is a hysteresis effect in the magnetization process originating from the slow magnetic relaxation, which makes it possible to store information in a single molecule.⁹ The second fascinating feature is that the relaxation of these magnetization shows clear quantum effect. Studies involving quantum tunneling of the magnetization³¹ and quan-

tum phase interference^{9a} have been conducted with the hope of using SMMs in quantum devices in the future. The first reported SMM was $[\text{Mn}_{12}\text{O}_{12}(\text{O}_2\text{CMe})_{16}(\text{H}_2\text{O})_4]$ ([Mn12]), and several analogues of [Mn12]³² and $[\text{Fe}_8\text{O}_2(\text{OH})_{12}(\text{tacn})_6]^{8+}$ (tacn = 1,4,7-triazacyclononane)³³ have since been extensively studied. While a number of SMMs containing manganese,³⁴ iron,³⁵ nickel,³⁶ vanadium,³⁷ and cobalt³⁸ ions have been reported, [Mn12] still has the highest blocking temperature SMM.

SMMs must have a large uniaxial magnetic anisotropy of easy axis type (large negative zero-field splitting parameter, $D < 0$) and a relatively large ground state spin multiplicity (S). The spin Hamiltonian can be written as

$$H = g\mu_B HS + D[S_z^2 - S(S+1)/3] + E(S_x^2 - S_y^2). \quad (2)$$

D and E represent uniaxial and rhombic zero-field splitting parameters, respectively. The first term represents the Zeeman energy, and the second term is the contribution from the magnetic anisotropy of D . In zero applied field, the energy levels of S in SMMs can be described as a symmetrical double minimum potential (Fig. 6a), where E term was ignored. Since D is negative, the $m_s = \pm S$ levels will be the lowest, and all the levels ($-S \leq m_s \leq +S$) are degenerated, except $m_s = 0$ in the case of integer spin system, and two potential minimum are equally populated before external magnetic field is applied. The energy barrier, which is the difference in energy between $m_s = \pm S$ states and the highest one(s), can be expressed as $\Delta E = |D|S_z^2$ for integer spin systems, and $\Delta E = |D|(S_z^2 - 1/4)$ for half-integer spin systems. When a magnetic field is applied parallel to the easy axis, the ground state degeneracy is removed and at low temperature only $m_s = -S$ state will be populated (magnetization was saturated) (Fig. 6b). After the applied magnetic field is switched off, the magnetization decays to thermal equilibrium with thermally activated first-order kinetics, and the single relaxation process follows the Arrhenius law ($\tau = \tau_0 \exp(\Delta E/k_B T)$, where τ_0 is the pre-exponential factor and k_B is the Boltzmann constant) (Fig. 6c).

This magnetic relaxation will be very slow in the system with relatively large S and negative D values. Since the relaxation time becomes so long, stepped magnetic hysteresis is first observed in [Mn12]. The steps correspond to fields at which a rapid increase of the relaxation rate is observed, and this behavior originates from the quantum spin tunneling between pairs of crossing levels. In zero applied field, the lowest $m_s = \pm S$ levels are in the tunneling condition, and relaxation rate

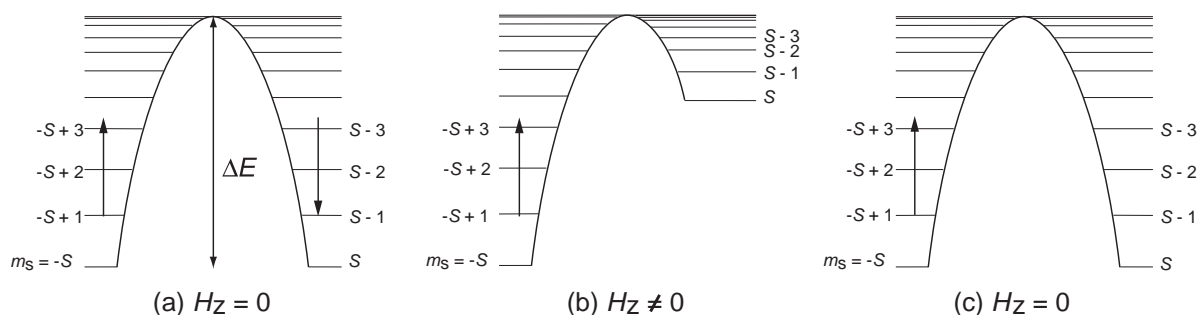


Fig. 6. Energy levels for a spin state S with easy axis magnetic anisotropy. a) In zero applied field the two ground states are equally populated. b) Under applied magnetic field, only left potential minimum are populated. c) After removing the magnetic field, the left potential minimum is still populated at very low temperature (spin flip is frozen).

becomes comparatively fast. In the presence of an external magnetic field along the easy axis of the molecules, mismatch of the energy levels leads to the absence of the quantum spin tunneling. However, the condition for tunneling is restored for fields, at which the $m_s = +n$ level has the same energy as of the $m_s = -n + m$ level, where n and m are any integer number, and the interval of such magnetic fields can be described as $\Delta H = D/g\mu_B$ when only uniaxial magnetic anisotropy is considered. In this account, we present the rational syntheses of SMMs and discuss the control of magnetic anisotropy.

Homo-Metal SMMs

In designing high-spin molecules, the symmetry of the magnetic orbitals and bridging structures should be carefully considered, and this was pointed out in the previous sections. Usually, homo-metal systems show antiferromagnetic interactions; however, metal ions bridged with a bond angle of 90° would have ferromagnetic interactions. It is already known that phenoxo and alkoxo groups sometime bridge metal ions without magnetic orbital overlap (bridging bond angle close to 90°), leading to ferromagnetic interactions. We have found that tridentate Schiff bases, prepared by condensation reactions of salicylaldehyde with aminoalkylalcohol, bridge to afford ferromagnetic interactions. We present here synthesis of homo-metal SMMs by using Schiff bases.

Ferrous Cube SMMs.³⁹ The reactions of $\text{FeCl}_2 \cdot 4\text{H}_2\text{O}$ with two types of tridentate bridging ligands H_2sap and H_2sae (Chart 3, H_2sap and H_2sae are salicylideneamino-1-propanol and salicylideneamino-1-ethanol, respectively) gave the fer-

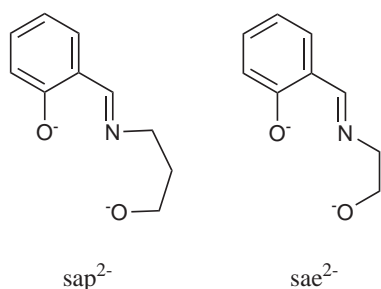


Chart 3.

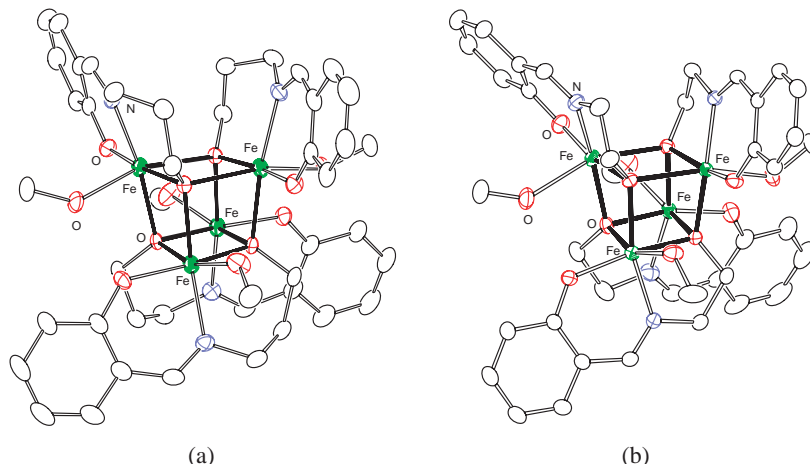
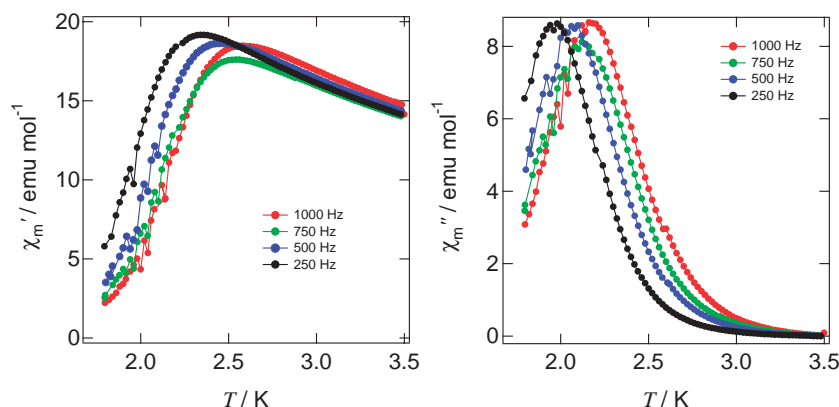


Fig. 7. Structures of (a) $[\text{Fe}^{\text{II}}_4(\text{sap})_4(\text{MeOH})_4]$ and (b) $[\text{Fe}^{\text{II}}_4(\text{sae})_4(\text{MeOH})_4]$.

rous cubes $[\text{Fe}^{\text{II}}_4(\text{sap})_4(\text{MeOH})_4]$ and $[\text{Fe}^{\text{II}}_4(\text{sae})_4(\text{MeOH})_4]$ (Fig. 7). The ferrous cubes have tetranuclear cubic core structures (Fig. 7). In the complexes, four Fe^{II} ions are bridged by μ_3 -alkoxo groups, giving an approximately cubic array of alternating iron and oxygen atoms. The Fe^{2+} ions have axially elongated coordination geometries. The elongated axis (axial axis) of the each Fe^{2+} ion lies perpendicular to the molecular S_4 axis, and elongated axis aligned orthogonally. The two cubes have subtle differences in coordination structures. The equatorial coordination bond lengths in $[\text{Fe}^{\text{II}}_4(\text{sae})_4(\text{MeOH})_4]$ are shorter than those in $[\text{Fe}^{\text{II}}_4(\text{sap})_4(\text{MeOH})_4]$, and the different coordination environments are due to the steric strain on the Fe^{2+} ions. The octahedrons about the Fe^{2+} ions in $[\text{Fe}^{\text{II}}_4(\text{sae})_4(\text{MeOH})_4]$ are more squeezed in the equatorial plane than those in $[\text{Fe}^{\text{II}}_4(\text{sap})_4(\text{MeOH})_4]$, and the differences in the Jahn–Teller distortion modes resulted in different ac susceptibility behaviors.

Ferrous cubes showed ferromagnetic behavior and have $S = 8$ spin ground states. The magnetizations did not show saturation up to 5 T, and the analyses of magnetization data gave positive ($D = +0.8 \text{ cm}^{-1}$) and negative (-0.76 cm^{-1}) zero-field splitting parameter for $[\text{Fe}^{\text{II}}_4(\text{sap})_4(\text{MeOH})_4]$ and $[\text{Fe}^{\text{II}}_4(\text{sae})_4(\text{MeOH})_4]$, respectively. From ac magnetic susceptibility measurements, $[\text{Fe}^{\text{II}}_4(\text{sae})_4(\text{MeOH})_4]$ showed frequency-dependent χ' and χ'' signals (Fig. 8), while the χ'' signal for $[\text{Fe}^{\text{II}}_4(\text{sap})_4(\text{MeOH})_4]$ was not observed down to 1.8 K. The temperature dependence of χ'' showed a peak maxima at 1.8–2.5 K, which shifted to a lower temperature as the ac frequency decreased from 1000 to 50 Hz. The Arrhenius plots derived from ac susceptibility data indicate that $[\text{Fe}^{\text{II}}_4(\text{sae})_4(\text{MeOH})_4]$ was an SMM with $\Delta E = 28 \text{ K}$ and pre-exponential factors (τ_0) of $3.63 \times 10^{-9} \text{ s}$. It is noted that $[\text{Fe}^{\text{II}}_4(\text{sap})_4(\text{MeOH})_4]$ is a non SMM, due to the molecule having positive D values.

We have prepared a variety of tridentate Schiff base ligands which are very useful for assembling metal ions in cubic structures, and homo-metal high-spin molecules should be systematically available. In addition, the present results gave an interesting subject about magnetic anisotropy of single-ions (D_{ion}) and molecules (D_{mol}). In the next section, we will propose possible control of magnetic anisotropy by chemical modifications.

Fig. 8. In- and out-of-phase ac signals for $[\text{Fe}^{\text{II}}_4(\text{sae})_4(\text{MeOH})_4]$.**Controlled Magnetic Anisotropy at Molecular Level.**⁴⁰

SMMs require high-spin ground states (S) and uniaxial magnetic anisotropy ($D < 0$) in cluster molecules. Although high-spin molecules can be rationally prepared, control of magnetic anisotropy is still a challenging subject. The sign of the D value relates to Jahn–Teller distortion (distortion of molecule), and simple ligand field approach gives some clues about control.⁴¹ Molecular magnetic anisotropy (D_{mol}) occurs due to several factors, including single-ion anisotropy of the constituent metal ions (D_{ion}), anisotropic exchange interactions between these ions, and magnetic dipolar interactions. Among them, D_{ion} often dominates D_{mol} . The ferrous cubes presented in the previous section have negative or positive D_{cube} values, which must be originating from D_{ion} of Fe^{2+} ions (D_{Fe}). We will discuss the origin of the different sign of D_{Fe} values in the ferrous cubes.

The sign of the D_{ion} values depends on the electron configuration and ligand field environment of a metal ion. When the orbital degeneracy is completely lifted in the electronic ground state under a low-symmetry ligand field, the Abragam–Pryce’s derivation of the spin Hamiltonian can be used to define the zero-field splitting as the quadratic forms of the spin operators including uniaxial D and rhombic E terms as described in Eqs. 3–5.⁴²

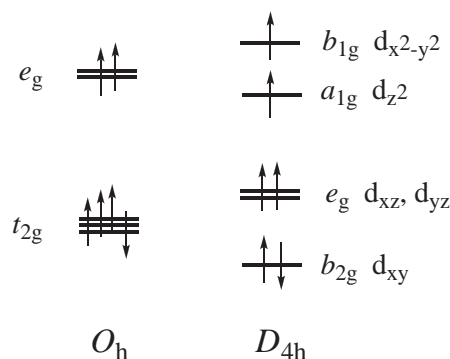
$$D = \lambda^2(\Lambda_{xx} + \Lambda_{yy} - 2\Lambda_{zz})/2, \quad (3)$$

$$E = \lambda^2(\Lambda_{xx} - \Lambda_{yy})/2, \quad (4)$$

$$\Lambda_{\alpha\beta} = \sum_{n \neq 0} \frac{\langle \varphi_0 | \hat{L}_\alpha | \varphi_n \rangle \langle \varphi_n | \hat{L}_\beta | \varphi_0 \rangle}{E_n - E_0}. \quad (5)$$

Parameters of λ and $\Lambda_{\alpha\beta}$ are the spin–orbit coupling constant and the mixing tensor of the ground and excited states, respectively. The sign of the D value depends upon the relative amplitude of $\Lambda_{\alpha\beta}$. These anisotropy terms originate from spin–orbit coupling $\lambda \mathbf{L} \cdot \mathbf{S}$, which mixes higher-energy multiplets into the ground state via second-order perturbations, and they dominate low-temperature magnetism of transition-metal complexes that are either easy-axis type with negative D and easy-plane type with positive D , respectively.

In a high-spin Fe^{2+} ion, tetragonal Jahn–Teller effects split the t_{2g} orbitals into the e_g and b_{2g} orbitals under D_{4h} symmetry, causing the 5E_g or ${}^5B_{2g}$ terms to become the ground state. The 5E_g or ${}^5B_{2g}$ states do not have orbital angular momentum, but

Scheme 6. d-Orbital splitting scheme under O_h and D_{4h} point groups.

mixing with the other states via spin–orbit coupling gives rise to magnetic anisotropies. The splitting of the t_{2g} orbitals depends on both π -donating and -accepting ability of the ligands, while π -back-donation in high-spin Fe^{2+} ions is assumed to be small. The d_{xz} and d_{yz} orbitals are, therefore, destabilized, and the b_{2g} orbital becomes the lowest in energy, while the ${}^5B_{2g}$ term becomes the ground state (Scheme 6).

The D_{ion} can be predicted by taking into account the crystal field generated by the ligands and by introducing the real geometry of the coordination sphere by using the angular-overlap model (AOM).⁴³ AOM is a ligand field model, which uses molecular orbital oriented e_σ and e_π parameters for each donor atom, and is particularly well suited to account for angular distortions in the ligand field. The energy splits in the ${}^5B_{2g}$ state of a single Fe^{2+} ion were calculated using AOM, and the calculated energy splitting scheme for a $3d^6$ system subjected to N_1O_5 coordination are shown in Fig. 9a, where the decrease in the p value from unity corresponds to the compressed octahedral coordination. If the π -donation from the equatorial ligands is weak ($p = 0.5$), the ${}^5B_{2g}$ term is not a good eigenstate, and it splits into two nearly degenerate states and one nondegenerate state. Calculations with a magnetic field along the y -axis gave a quasi-first-order Zeeman effect involving the low-lying nearly degenerate states, suggesting that the split states, where the equatorial π -donation is weak, correspond to the $m_s = \pm 2, \pm 1$, and 0 states in order from the lowest energy (Fig. 9b). The equatorial coordination bond lengths about the Fe^{2+} ions in $[\text{Fe}^{\text{II}}_4(\text{sae})_4(\text{MeOH})_4]$ are shorter than those for

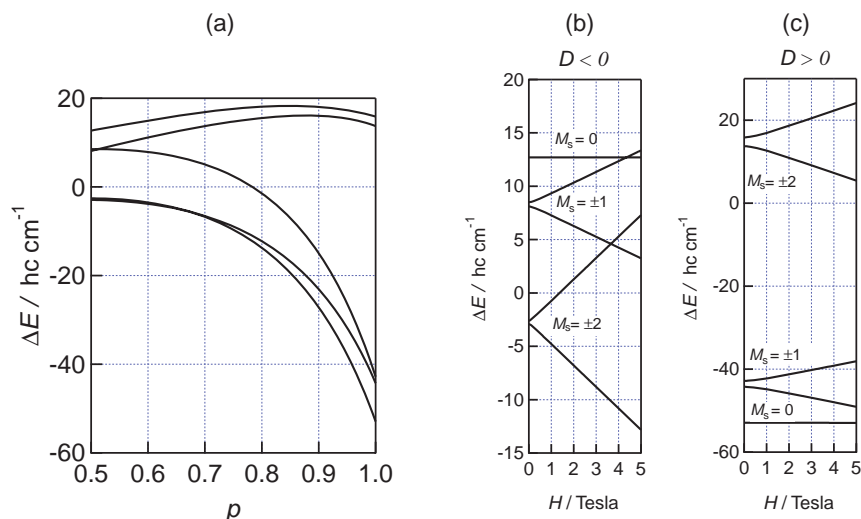
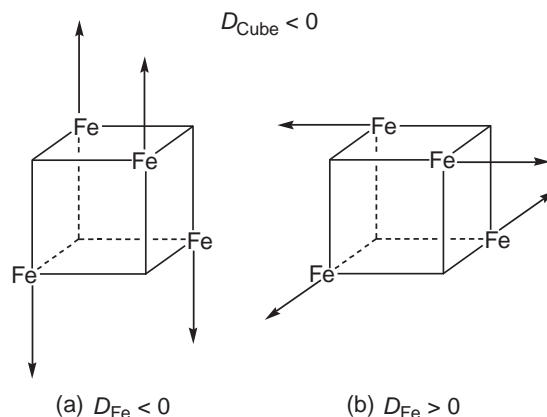


Fig. 9. (a) Energy splitting scheme of the ${}^5B_{2g}$ state calculated for an octahedral $3d^6$ system subjected to N_1O_5 coordination. The variable p changes the ligand field strengths of $e_\pi(//)$ and $e_\pi(\perp)$. Energy splitting schemes by the applied magnetic field parallel to the y -axis with (b) $p = 0.5$ and parallel to the x -axis with (c) $p = 1.0$.

$[\text{Fe}^{\text{II}}_4(\text{sap})_4(\text{MeOH})_4]$, meaning that the coordination spheres of the Fe^{2+} ions in $[\text{Fe}^{\text{II}}_4(\text{sae})_4(\text{MeOH})_4]$ are equatorially more compressed than those in $[\text{Fe}^{\text{II}}_4(\text{sap})_4(\text{MeOH})_4]$, and the π -donation from the equatorial sites to the Fe^{2+} ions in $[\text{Fe}^{\text{II}}_4(\text{sae})_4(\text{MeOH})_4]$ is stronger. Therefore, the Fe^{2+} ions in $[\text{Fe}^{\text{II}}_4(\text{sap})_4(\text{MeOH})_4]$ have negative D_{Fe} values. When the equatorial π -donation is strong ($p = 1$), the ${}^5B_{2g}$ state is split into five states, and the two sets of the higher energy states show Zeeman splits by the magnetic field along the x -axis (Fig. 9c). The lowest state was assigned to the $m_s = 0$ state, which corresponds to the positive value of D_{Fe} for the Fe^{2+} ion in $[\text{Fe}^{\text{II}}_4(\text{sae})_4(\text{MeOH})_4]$. Consequently, the value of D_{Fe} changes its sign from the positive to negative as the equatorial π -donation becomes weaker caused by the slight structural change in coordinating ligands. The obtained results suggest that the single ion magnetic anisotropy can be controlled by simple chemical modifications. In the next section, we discuss how D_{mol} arises from D_{ion} .

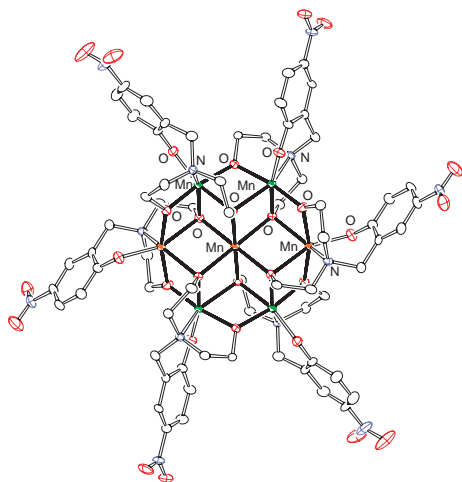
Molecular Magnetic Anisotropy. Magnetically anisotropic high-spin molecules can have either negative or positive D_{mol} values, and the sign of the D_{mol} value depends upon how the anisotropic metal ions are assembled in a molecule. Although the parameter D_{mol} is generally provided by a tensorial sum over constituent ions for a strong coupling limit,^{44,45} more intuitive approaches useful for molecular design will be discussed here. Based on a classical vector picture, molecules with negative values of D_{mol} have two possible origins: (i) a collinear easy-axis alignment or (ii) an orthogonal hard-axis alignment of anisotropic single ions.^{36,46} The ferrous cube, $[\text{Fe}^{\text{II}}_4(\text{sae})_4(\text{MeOH})_4]$, is a typical example of latter case (Scheme 7b). The metal cube has S_4 symmetry, and four single-ion spins are ferromagnetically coupled such that their quantization axes are mutually orthogonal and $D_{\text{mol}} = -(1/8)D_{\text{Fe}}$. It can be expected that the metal ion assemblage with mutually orthogonal single-ion quantization axes induces a sign inversion of uniaxial magnetic anisotropy in a molecule, i.e., orthogonal hard- and easy-axis alignments of the component metal ions give easy- and hard-axis anisotropy for mole-



Scheme 7. (a) Collinear easy-axis ($D_{\text{Fe}} < 0$) and (b) orthogonal hard-axis ($D_{\text{Fe}} > 0$) alignments required for the negative D_{cube} value.

cules, respectively. This strategy can be extended to larger molecules and used to predict the sign of the D_{mol} values. Collinear easy axis and orthogonal hard axis alignments give negative D_{mol} values (Scheme 7). In the case of $[\text{Fe}^{\text{II}}_4(\text{sae})_4(\text{MeOH})_4]$, which shows orthogonal alignment of hard axis ($D_{\text{Fe}} > 0$), the magnetic anisotropy of the cubes D_{cube} become negative (Scheme 7b). In $[\text{Fe}^{\text{II}}_4(\text{sap})_4(\text{MeOH})_4]$, Fe^{2+} ions with negative D_{Fe} values are aligned in such a way to give positive D_{cube} values. This result suggests that simple chemical modifications of the bridging ligands can control D_{ion} , followed by D_{mol} .

$\text{Mn}^{\text{III}}_4\text{Mn}^{\text{II}}_3$ Mixed-Valent Wheel SMM.⁴⁷ The reaction of a reduced Schiff base ligand ($\text{H}_3\text{L}1 = N$ -(2-hydroxy-5-nitrobenzyl)iminodiethanol) with MnCl_2 yielded dark red crystals of $[\text{Mn}^{\text{II}}_3\text{Mn}^{\text{III}}_4\text{L}1_6] \cdot 7\text{C}_2\text{H}_4\text{Cl}_2$ (Fig. 10). The seven manganese ions linked by six trianionic ligands ($\text{L}1^{3-}$) form the wheel structure, which has three Mn^{2+} ions on the rim and one in the center and the other four Mn^{3+} ions on the rim. $\chi_{\text{m}}T$ values of the complex increased with decreasing temper-

Fig. 10. Structure of $[\text{Mn}^{\text{II}}_3\text{Mn}^{\text{III}}_4\text{L}_{16}]$.

ature and reached a maximum value of $53.9 \text{ emu mol}^{-1} \text{ K}$ at 7.0 K , which suggests molecule has substantial high-spin ground states. S value of $[\text{Mn}^{\text{II}}_3\text{Mn}^{\text{III}}_4\text{L}_{16}]$ is in the range of $31/2$ – $1/2$. Magnetization data suggested that $[\text{Mn}^{\text{II}}_3\text{Mn}^{\text{III}}_4\text{L}_{16}]$ has a spin ground state of $S = 19/2$ or $17/2$ with negative D values. The relatively high-spin ground state in $[\text{Mn}^{\text{II}}_3\text{Mn}^{\text{III}}_4\text{L}_{16}]$ originates from the ferrimagnetic spin ground state by ferro- and antiferromagnetic interactions between Mn^{2+} and Mn^{3+} ions. It should be mentioned that $[\text{Mn}^{\text{II}}_3\text{Mn}^{\text{III}}_4\text{L}_{16}]$ is a mixed-valent wheel SMM with $\Delta E = 18.1 \text{ K}$.

Hetero-Metal SMM

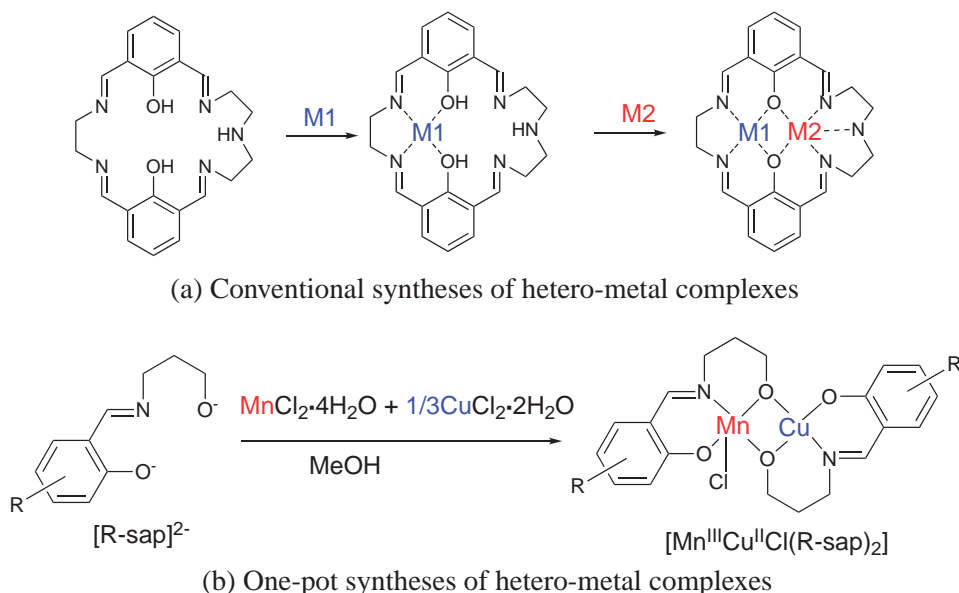
Facile One-Pot Syntheses of Hetero-Metal Complexes.

A combination of different metal ions is a possible way to prepare molecules with larger magnetic anisotropy and higher-spin ground states by ferro- or antiferromagnetic interactions. A cyanide-bridged single-molecule magnet of $\text{K}[(\text{L})_6\text{MnMo}_6(\text{CN})_{18}](\text{ClO}_4)_3$ ($\text{L} = N,N',N''$ -trimethyl-1,4,7-triazacyclononane),⁴⁸ and some hetero-metal SMMs composed of d – d ⁴⁹

and d – f ⁵⁰ spins were recently reported. However, the number of hetero-metal SMMs is still limited, even though SMMs will lead to an understanding of quantum tunneling effects through synergy of hetero-metal spins. This might be caused by the complexity of the synthetic procedure for hetero-metal complexes. A well-known synthetic path for hetero-metal systems contains step-by-step reactions of different metal ions with ligands, such as macro-cycles (Scheme 8a).⁵¹ In this synthetic method, it is necessary to prepare specific ligands with multi-coordination sites, in which each coordination sites exhibit different affinity for metal ions. In this context, we have established a facile one-pot synthetic way to hetero-metal complexes as shown in Scheme 8b. This synthesis can afford various hetero-metal complexes by just reacting different metal ions with simple tridentate ligands. In the reactions, slight differences in the consecutive stability constants between metal ions and the ligands afford to achieve the selective formation of hetero-metal complexes. In the next section, we will present novel one-pot syntheses of hetero-metal SMMs.

A Dinuclear Mn^{III} – Cu^{II} SMM.⁵² A molecule with the high-spin ground state can be prepared by arranging metal ions orthogonally with respect to their magnetic orbitals. Mn^{3+} and Cu^{2+} ions, each having no spin and unpaired spin on $d_{x^2-y^2}$ orbitals, respectively, might be a suitable combination to cause ferromagnetic interactions by strict orthogonality. Additionally, a Mn^{3+} ion exhibits uniaxial magnetic anisotropy, and it is expected to introduce magnetic anisotropy to the molecules.

Reaction of $1/3$ equivalent of $\text{CuCl}_2 \cdot 2\text{H}_2\text{O}$ with $\text{MnCl}_2 \cdot 4\text{H}_2\text{O}$ and Schiff base ligand 5-bromo-2-salicylideneamino-1-propanol ($\text{H}_2\text{5-Br-sap}$) in methanol gave dark brown crystals of $[\text{Mn}^{\text{III}}\text{Cu}^{\text{II}}\text{Cl}(\text{5-Br-sap})_2(\text{MeOH})]$ (Fig. 11a), which has a dinuclear structure composed of Mn^{3+} and Cu^{2+} ions doubly bridged by two alkoxo groups. Dc magnetic susceptibility measurements showed ferromagnetic behavior with best fitting parameters of $J_{\text{MnCu}} = 78 \text{ cm}^{-1}$ and $D = -1.86 \text{ cm}^{-1}$ for the $S = 5/2$ spin ground state. The fairly strong ferromagnetic interactions between Mn^{3+} and Cu^{2+} ions can be understood by



Scheme 8.

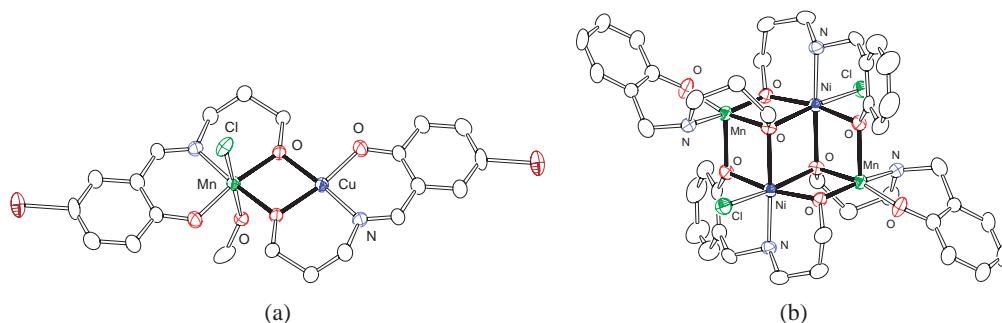


Fig. 11. Structures of $[\text{Mn}^{\text{III}}\text{Cu}^{\text{II}}\text{Cl}(\text{5-Br-sap})_2(\text{MeOH})]$ and $[\text{Mn}^{\text{III}}_2\text{Ni}^{\text{II}}_2\text{Cl}_2(\text{L2})_4]$.

the strict orthogonality of their magnetic orbitals. The Mn^{3+} ion under tetragonally elongated octahedral coordination geometry has four unpaired electrons on the e_g (d_{xz} and d_{yz}), b_{2g} (d_{xy}), and a_{1g} (d_{z^2}), which are orthogonal to the $d_{x^2-y^2}$ orbital on the square-planar Cu^{2+} ion (d^9). The evidence for slow relaxation of magnetization can be obtained by ac magnetic susceptibility measurements. The ac magnetic susceptibility data down to 26 mK confirmed that $[\text{Mn}^{\text{III}}\text{Cu}^{\text{II}}\text{Cl}(\text{5-Br-sap})_2(\text{MeOH})]$ is an SMM with $\Delta E = 10.5$ K.

A Tetranuclear $\text{Mn}^{\text{III}}_2\text{Ni}^{\text{II}}_2$ SMM.⁵³ Our synthetic method for hetero-metal complexes is also applicable to other combinations of metal ions. A reaction of 1:1 mixtures of L2 ($\text{H}_2\text{L2} = N$ -(2-hydroxybenzyl)-3-amino-1-propanol) with $\text{MnCl}_2 \cdot 4\text{H}_2\text{O}$ and $\text{NiCl}_2 \cdot n\text{H}_2\text{O}$ in methanol gave dark-red crystals of $[\text{Mn}^{\text{III}}_2\text{Ni}^{\text{II}}_2\text{Cl}_2(\text{L2})_4]$ in high yield. The structure consists of an incomplete face-sharing double cube with two Mn^{3+} and two Ni^{2+} ions (Fig. 11b). The Mn^{3+} and Ni^{2+} ions are doubly bridged to form a dinuclear unit by two alkoxo groups, and the symmetrically related dinuclear units are bridged by phenoxo and alkoxo groups in μ_2 and μ_3 fashions, respectively. Dc magnetic susceptibility measurements showed ferromagnetic behavior, and the analyses of the magnetic susceptibility and magnetization data gave the best fitting parameters of J_{MnNi} , J_{MnNi^*} , J_{NiNi^*} , and D being 4.5(1), 4.3(1), $-7.9(2)$, and $-0.85(1) \text{ cm}^{-1}$, respectively. SMM characteristic was confirmed by ac susceptibility measurements, and a stepped hysteresis was observed at 0.55 K.

The present synthetic method is versatile for assembling hetero-metal ions. This method is also expected to be applicable to prepare SMMs with higher nuclearities and 3d-4f hetero-metal systems by chemical modifications of bridging ligands.

Conclusion

In this paper, we present rational syntheses of high-spin molecules including SMMs. We have been working to prepare high-spin molecules since the late 80's and throughout 90's, and a new era of SMMs began in 1993. We have applied our synthetic strategy to prepare SMMs. Although many SMMs have been prepared, they were obtained accidentally and mechanisms related to quantum spin dynamics in SMMs, for example, effects of spin topologies on the tunnelling gap, are not yet fully understood. Chemistry of large paramagnetic molecules showing quantum phenomena is just at the beginning, and new cluster molecules help to explore and develop new fields of high-spin chemistry. We believe that our syn-

thetic strategies of high-spin molecules will be important for developing studies on new quantum effects in multi-nuclear metal complexes.

References

- 1 a) C. Kollmar, O. Kahn, *Acc. Chem. Res.* **1993**, 26, 259. b) J. S. Miller, A. J. Epstein, *Angew. Chem., Int. Ed. Engl.* **1994**, 33, 385.
- 2 a) O. Kahn, J. Galy, Y. Journaux, J. Jaud, I. Morgenstern-Badarau, *J. Am. Chem. Soc.* **1982**, 104, 2165. b) Y. Pei, Y. Journaux, O. Kahn, *Inorg. Chem.* **1989**, 28, 100. c) A. Caneschi, D. Gatteschi, J. Laugier, P. Rey, *J. Am. Chem. Soc.* **1987**, 109, 2191. d) H. Tamaki, Z. J. Zhong, N. Matsumoto, S. Kida, M. Koikawa, N. Achiwa, Y. Hashimoto, S. Okawa, *J. Am. Chem. Soc.* **1992**, 114, 6974. e) H. Oshio, U. Nagashima, *Inorg. Chem.* **1992**, 31, 3295.
- 3 a) J. S. Miller, J. C. Calabrese, H. Rommelmann, R. Chittipeddi, J. H. Zhang, W. M. Reiff, A. J. Epstein, *J. Am. Chem. Soc.* **1987**, 109, 769. b) P. Turek, K. Nozawa, D. Shimoi, K. Awaga, T. Inabe, Y. Maruyama, M. Kinoshita, *Chem. Phys. Lett.* **1991**, 180, 327.
- 4 a) K. Itoh, *Chem. Phys. Lett.* **1967**, 1, 235. b) T. Sugawara, S. Bandow, K. Kimura, H. Iwamura, K. Itoh, *J. Am. Chem. Soc.* **1986**, 108, 368. c) Y. Teki, T. Takui, K. Itoh, H. Iwamura, K. Kobayashi, *J. Am. Chem. Soc.* **1986**, 108, 2147. d) I. Fujita, Y. Teki, T. Takui, T. Kinoshita, K. Itoh, *J. Am. Chem. Soc.* **1990**, 112, 4074.
- 5 H. M. McConnell, *J. Chem. Phys.* **1963**, 39, 1910.
- 6 a) J. S. Miller, A. J. Epstein, W. M. Reiff, *Acc. Chem. Res.* **1988**, 21, 114, references therein. b) C. Kollmar, M. Vouty, O. Kahn, *J. Am. Chem. Soc.* **1991**, 113, 7994. c) A. Izuoka, S. Murata, T. Sugawara, H. Iwamura, *J. Am. Chem. Soc.* **1987**, 109, 2631.
- 7 a) R. Sessoli, D. Gatteschi, A. Caneschi, M. A. Novak, *Nature* **1993**, 365, 141. b) R. Sessoli, H.-L. Tsai, A. R. Schake, S. Wang, J. B. Vincent, K. Folting, D. Gatteschi, G. Christou, D. N. Hendrickson, *J. Am. Chem. Soc.* **1993**, 115, 1804.
- 8 G. Christou, D. Gatteschi, D. N. Hendrickson, R. Sessoli, *MRS Bull.* **2000**, 25, 66.
- 9 a) W. Wernsdorfer, R. Sessoli, *Science* **1999**, 284, 133. b) M. N. Leuenberger, D. Loss, *Nature* **2001**, 410, 789. c) M. Clemente-León, R. Coronado, A. Forment-Aliaga, P. Amoros, J. Ramirez-Calbet, *J. Mater. Chem.* **2003**, 13, 3089. d) A. Cornia, A. C. Fabretti, M. Pacchioni, L. Zoppi, D. Bonacchi, A. Caneschi, D. Gatteschi, R. Biagi, U. Del Pennino, V. De Renzi, L. Gurevichi, H. S. J. Van der Zant, *Angew. Chem., Int. Ed.* **2003**, 42, 1645.

- 10 a) H. Oshio, T. Watanabe, A. Ohto, T. Ito, U. Nagashima, *Angew. Chem., Int. Ed. Engl.* **1994**, *33*, 670. b) H. Oshio, T. Watanabe, A. Ohto, T. Ito, T. Ikoma, S. Tero-Kubota, *Inorg. Chem.* **1997**, *36*, 3014.
- 11 a) G. A. Fox, C. G. Pierpont, *Inorg. Chem.* **1992**, *31*, 3718. b) G. A. Abakumov, V. K. Cherkasov, M. P. Bubnov, O. G. Ellert, U. V. Rakitin, L. N. Zakharov, Y. T. Struchkov, U. N. Saf'yanov, *Isv. Akad. Nauk SSSR* **1992**, 2315.
- 12 C. W. Lange, B. J. Conklin, C. G. Pierpont, *Inorg. Chem.* **1994**, *33*, 1276.
- 13 a) D. M. Adams, A. L. Rheingold, A. Dei, D. N. Hendrickson, *Angew. Chem., Int. Ed. Engl.* **1993**, *32*, 391. b) A. Ozarowski, B. R. McGarvey, A. El-Hadad, Z. Tian, D. G. Tuck, D. J. Krovich, G. C. DeFotis, *Inorg. Chem.* **1993**, *32*, 841.
- 14 S. Bruni, A. Caneschi, F. Cariati, C. Delfs, A. Dei, D. Gatteschi, *J. Am. Chem. Soc.* **1994**, *116*, 1388.
- 15 F. A. Cotton, G. Wilkinson, *Advanced Inorganic Chemistry*, 5th ed., Wiley, New York, **1988**.
- 16 E. Müller, C. Piguet, G. Bernardinelli, A. F. Williams, *Inorg. Chem.* **1988**, *27*, 849.
- 17 a) M. Moscherosch, J. S. Field, W. Kaim, S. Kohlmann, M. Krejčík, *J. Chem. Soc., Dalton Trans.* **1993**, 211. b) C. Vogler, H.-D. Hausen, W. Kaim, S. Kohlmann, H. E. A. Kramer, J. Rieker, *Angew. Chem.* **1989**, *101*, 1734.
- 18 a) O. Kahn, *Molecular Magnetism*, VCH Publishers, Weinheim, New York, **1993**. b) I. Seggern, F. Tuczek, W. Bensch, *Inorg. Chem.* **1995**, *34*, 5530. c) F. Tuczek, E. I. Solomon, *J. Am. Chem. Soc.* **1994**, *116*, 6916.
- 19 J. B. Goodenough, *Magnetism and Chemical Bond*, Interscience, New York, **1963**.
- 20 M. Tamura, Y. Nakazawa, D. Shiomi, K. Nozawa, Y. Hosokoshi, M. Ishioka, M. Takahashi, M. Kinoshita, *Chem. Phys. Lett.* **1991**, *186*, 401.
- 21 R. Hotzelmann, K. Wieghardt, U. Flörke, H.-J. Haupt, D. C. Weatherburn, J. Bonvoisin, G. Blondin, J.-J. Gierard, *J. Am. Chem. Soc.* **1992**, *114*, 1681.
- 22 M. Andruh, I. Ramade, E. Codjovi, O. Guillou, O. Kahn, J. C. Trombe, *J. Am. Chem. Soc.* **1993**, *115*, 1822.
- 23 a) H. M. McConnell, *Proc. Robert A. Welch Found. Conf. Chem. Res.* **1976**, *11*, 144. b) R. Breslow, B. Juan, R. Q. Klutetz, C. Z. Xia, *Tetrahedron* **1982**, *38*, 863. c) R. Breslow, *Pure Appl. Chem.* **1982**, *54*, 927.
- 24 a) F. Tuczek, E. I. Solomon, *Inorg. Chem.* **1993**, *32*, 2850. b) Z. Shen, J. W. Allen, J. J. Yeh, J.-S. Kang, W. Ellis, W. Spicer, I. Lindau, M. B. Maple, Y. D. Dalichaouch, M. S. Torikachvili, J. Z. Sun, T. H. Geballe, *Phys. Rev. B* **1987**, *36*, 8414.
- 25 H. Oshio, A. Ohto, T. Ito, *Chem. Commun.* **1996**, 1541.
- 26 H. Oshio, T. Kikuchi, T. Ito, *Inorg. Chem.* **1996**, *35*, 4938.
- 27 H. Oshio, H. Okamoto, T. Kikuchi, T. Ito, *Inorg. Chem.* **1997**, *36*, 3201.
- 28 a) H. M. McConnell, *J. Chem. Phys.* **1963**, *31*, 299. b) N. Mataga, *Theor. Chim. Acta* **1968**, *10*, 372. c) A. A. Ovchinnikov, *Theor. Chim. Acta* **1978**, *47*, 297. d) K. Itoh, *Pure Appl. Chem.* **1978**, *50*, 1251.
- 29 a) H. Oshio, H. Ichida, *J. Phys. Chem.* **1995**, *99*, 3294. b) H. Oshio, *J. Chem. Soc., Chem. Commun.* **1991**, 240.
- 30 a) J. R. Friedman, M. P. Sarachik, J. Tejada, R. Ziolo, *Phys. Rev. Lett.* **1996**, *76*, 3830. b) L. Thomas, L. Lioni, R. Ballou, D. Gatteschi, R. Sessoli, B. Barbara, *Nature* **1996**, *383*, 145. c) J. Tejada, R. F. Ziolo, X. X. Zhang, *Chem. Mater.* **1996**, *8*, 1784. d) S. M. Aubin, N. R. Gilley, L. Pardi, J. Krzystek, M. W. Wemple, L. C. Brunel, M. B. Maple, G. Christou, D. N. Hendrickson, *J. Am. Chem. Soc.* **1998**, *120*, 4991.
- 31 a) D. Gatteschi, A. Caneschi, L. Pardi, R. Sessoli, *Science* **1994**, *265*, 1054. b) A. Müller, F. Peters, M. T. Pope, D. Gatteschi, *Chem. Rev.* **1998**, *98*, 239. c) S. Hill, R. S. Edward, N. Aliaga-Alcalde, G. Christou, *Science* **2003**, *302*, 1015.
- 32 a) H. R. Friedman, M. P. Sarachik, J. Tejada, J. Maciejewski, R. Ziolo, *J. Appl. Phys.* **1996**, *79*, 6031. b) H. J. Eppley, H.-L. Tsai, N. De Vries, K. Folting, G. Christou, D. N. Hendrickson, *J. Am. Chem. Soc.* **1995**, *117*, 301. c) C. Boskovic, M. Pink, J. C. Huffman, D. N. Hendrickson, G. Christou, *J. Am. Chem. Soc.* **2001**, *123*, 9914.
- 33 a) D. Gatteschi, R. Sessoli, A. Cornia, *Chem. Commun.* **2000**, 725. b) A. L. Barra, P. Debrunner, D. Gatteschi, C. E. Schülux, R. Sessoli, *Eurphys. Lett.* **1996**, *35*, 133. c) Y. Pontillon, A. Caneschi, D. Gatteschi, R. Sessoli, E. Ressouche, J. Schweizer, E. Lelievre-Vera, *J. Am. Chem. Soc.* **1999**, *121*, 5342.
- 34 a) M. Soler, W. Wernsdorfer, K. A. Abboud, J. C. Huffman, E. R. Davidson, D. N. Hendrickson, G. Christou, *J. Am. Chem. Soc.* **2003**, *125*, 3576. b) C. Boskovic, E. K. Brehin, W. E. Streib, K. Folting, J. C. Bollinger, D. N. Hendrickson, G. Christou, *J. Am. Chem. Soc.* **2002**, *124*, 3725. c) E. K. Brehin, C. Boskovic, W. Wernsdorfer, J. Yoo, A. Yamaguchi, E. C. Sanudo, T. R. Concolino, A. L. Rheingold, H. Ishimoto, D. N. Hendrickson, G. Christou, *J. Am. Chem. Soc.* **2002**, *124*, 9710. d) W. Wernsdorfer, N. Aliaga-Alcalde, D. N. Hendrickson, G. Christou, *Nature* **2002**, *416*, 406. e) G. Aromi, S. Bhaduri, P. Artus, K. Folting, G. Christou, *Inorg. Chem.* **2002**, *41*, 805. f) C. Boskovic, E. K. Brehin, W. E. Streib, K. Folting, J. C. Bollinger, D. N. Hendrickson, G. Christou, *J. Am. Chem. Soc.* **2002**, *124*, 3725. g) J. Price, S. R. Batten, B. Moubaraki, K. S. Murray, *Chem. Commun.* **2002**, 762. h) J. T. Brockman, J. C. Huffman, G. Christou, *Angew. Chem., Int. Ed.* **2002**, *41*, 2506. i) M. Soler, P. Artus, K. Folting, J. C. Huffman, D. N. Hendrickson, G. Christou, *Inorg. Chem.* **2001**, *40*, 4902. j) N. Aliaga, K. Folting, D. N. Hendrickson, G. Christou, *Polyhedron* **2001**, *20*, 1273. k) H. Andres, R. Basler, H.-U. Gudel, G. Aromi, G. Christou, H. Buttner, B. Ruffe, *J. Am. Chem. Soc.* **2000**, *122*, 12469. l) P. Artus, C. Boskovic, J. Yoo, W. E. Streib, L.-C. Brunel, D. N. Hendrickson, G. Christou, *Inorg. Chem.* **2001**, *40*, 4199. m) M. Soler, E. Rumberger, K. Folting, D. N. Hendrickson, G. Christou, *Polyhedron* **2001**, *20*, 1365. n) S. M. Aubin, Z. Sun, L. Pardi, J. Krzystek, K. Folting, L.-C. Brunel, A. L. Rheingold, G. Christou, D. N. Hendrickson, *Inorg. Chem.* **1999**, *38*, 5329. o) S. M. Aubin, M. W. Wemple, D. M. Adams, H.-L. Tsai, G. Christou, D. N. Hendrickson, *J. Am. Chem. Soc.* **1996**, *118*, 7746. p) H. Miyasaka, R. Clérac, W. Wernsdorfer, L. Lecren, C. Bonhomme, K. Sugiura, M. Yamashita, *Angew. Chem., Int. Ed.* **2004**, *43*, 2801. q) M. Murugesu, J. Raftery, W. Wernsdorfer, G. Christou, E. K. Brehin, *Inorg. Chem.* **2004**, *43*, 4203. r) M. Murugesu, M. Habrych, W. Wernsdorfer, K. A. Abboud, G. Christou, *J. Am. Chem. Soc.* **2004**, *126*, 4766. s) A. J. Tasiopoulos, A. Vinslava, W. Wernsdorfer, K. A. Abboud, G. Christou, *Angew. Chem., Int. Ed.* **2004**, *43*, 2117.
- 35 a) C. Sangregorio, T. Ohm, C. Paulsen, R. Sessoli, D. Gatteschi, *Phys. Rev. Lett.* **1997**, *78*, 4645. b) H. Oshio, N. Hoshino, T. Ito, *J. Am. Chem. Soc.* **2000**, *122*, 12602. c) A. L. Barra, A. Caneschi, A. Cornia, F. de Biani, D. Gatteschi, C. Sangregorio, R. Sessoli, L. Sorace, *J. Am. Chem. Soc.* **1999**, *121*, 5302.
- 36 C. Cadiou, M. Murrie, C. Paulsen, V. Villar, W. Wernsdorfer, R. E. P. Winpenney, *Chem. Commun.* **2001**, 2666.
- 37 S. L. Castro, Z. Sun, C. M. Grant, J. C. Bollinger, D. N.

Hendrickson, G. Christou, *J. Am. Chem. Soc.* **1998**, *120*, 2365.

38 E. Yang, D. N. Hendrickson, W. Wernsdorfer, M. Nakano, L. N. Zakharov, R. D. Sommer, A. L. Rheingold, M. Ledezma-Gairaud, G. Christou, *J. Appl. Phys.* **2002**, *91*, 7382.

39 H. Oshio, N. Hoshino, T. Ito, *J. Am. Chem. Soc.* **2000**, *122*, 12602.

40 H. Oshio, N. Hoshino, T. Ito, M. Nakano, *J. Am. Chem. Soc.* **2004**, *126*, 8805.

41 D. Gatteschi, L. Sorace, *J. Solid State Chem.* **2001**, *159*, 253.

42 A. Abragam, B. Bleaney, *Electron Paramagnetic Resonance of Transition Ions*, Oxford University Press, **1970**, Sect. 19.2.

43 a) B. N. Figgis, M. A. Hitchman, *Ligand Field Theory and Its Applications*, Wiley-VCH, **2000**, Chap. 3. b) T. Schönher, *Top. Curr. Chem.* **1997**, *191*, 88. c) P. E. Hoggard, *Coord. Chem. Rev.* **1986**, *70*, 85. d) A. B. P. Lever, *Inorganic Electronic Spectroscopy*, 2nd ed., Elsevier, **1984**. e) E. Larsen, G. N. La Mar, *J. Chem. Educ.* **1974**, *51*, 633. f) J. K. Burdett, *Molecular Shapes*, John-Wiley & Sons, **1980**.

44 a) A. Bencini, D. Gatteschi, *Electron Paramagnetic Resonance of Exchange Coupled Systems*, Springer-Verlag, **1990**, Sect. 3.2 and 4.3. b) C. J. Ballhausen, *Introduction to Ligand Field Theory*, MacGraw-Hill, **1962**, Sect. 6-g.

45 a) A. Cornia, M. Affronte, A. G. M. Jansen, G. L. Abbati, D. Gatteschi, *Angew. Chem., Int. Ed.* **1999**, *38*, 2264. b) O. Waldmann, J. Schülein, R. Koch, P. Müller, I. Bernt, R. W. Saalfrank, H. P. Andres, H. U. Güdel, P. Allenspach, *Inorg. Chem.* **1999**, *38*, 5879. c) O. Waldmann, R. Koch, S. Schromm, J. Schülein, P. Müller, I. Bernt, R. W. Saalfrank, F. Hmpel,

E. Balthes, *Inorg. Chem.* **2001**, *40*, 2986. d) G. L. Abbati, L.-C. Brunel, H. Casalta, A. Cornia, A. C. Fabretti, D. Gatteschi, A. K. Hassan, A. G. M. Jansen, A. L. Maniero, L. Pardi, C. Paulsen, U. Serge, *Chem. Eur. J.* **2001**, *7*, 1796. e) D. Collison, V. S. Oganessian, S. Poligkos, A. J. Thomson, R. E. P. Winpenny, E. J. L. McInnes, *J. Am. Chem. Soc.* **2003**, *125*, 1168.

46 M. Nakano, G. Matsubayashi, T. Muramatsu, T. C. Kobayashi, K. Amaya, J. Yoo, G. Christou, D. N. Hendrickson, *Mol. Cryst. Liq. Cryst.* **2002**, *376*, 405.

47 S. Koizumi, M. Nihei, M. Nakano, H. Oshio, *Inorg. Chem.* **2005**, *44*, 1208.

48 J. J. Sokol, A. G. Hee, J. R. Long, *J. Am. Chem. Soc.* **2002**, *124*, 7656.

49 a) E. J. Schelter, A. V. Prosvirin, K. R. Dumber, *J. Am. Chem. Soc.* **2004**, *126*, 15004. b) H. J. Choi, J. J. Sokol, J. R. Long, *Inorg. Chem.* **2004**, *43*, 1606.

50 a) S. Osa, T. Kido, N. Matsumoto, N. Re, A. Oichaba, J. Mrozinski, *J. Am. Chem. Soc.* **2004**, *126*, 420. b) C. M. Zaleski, E. C. Depperman, J. W. Kampf, M. L. Kirk, V. L. Pecoraro, *Angew. Chem., Int. Ed.* **2004**, *43*, 3912. c) A. Mishra, W. Wernsdorfer, K. A. Abboud, G. Christou, *J. Am. Chem. Soc.* **2004**, *126*, 15648. d) J.-P. Costes, F. Dahan, W. Wernsdorfer, *Inorg. Chem.* **2006**, *45*, 5.

51 H. Ōkawa, H. Frutachi, D. E. Fenton, *Coord. Chem. Rev.* **1998**, *174*, 51.

52 H. Oshio, M. Nihei, A. Yoshida, H. Nojiri, M. Nakano, A. Yamaguchi, Y. Karaki, H. Ishimoto, *Chem. Eur. J.* **2005**, *11*, 843.

53 H. Oshio, M. Nihei, S. Koizumi, T. Shiga, H. Nojiri, M. Nakano, N. Shirakawa, M. Akatsu, *J. Am. Chem. Soc.* **2005**, *127*, 4568.



Award recipient

Hiroki Oshio was born in 1953 in Fukuoka. He graduated from Kyushu University in 1977 and received his Ph.D. in 1982 under the guidance of Professor Yoshimasa Takashima. He worked with Prof. Kazuo Nakamoto at Marquette University as a postdoctoral fellow in 1982–1984. He was pointed as a research associate at Institute for Molecular Science in 1985. He joined Professor Tasuku Ito's group at Department of Chemistry, Faculty of Science, Tohoku University in 1992 as an Associate Professor. From 2001, he has been a Professor in the Graduate School of Pure and Applied Sciences, Department of Chemistry, University of Tsukuba. His research interest focus on solid-state chemistry of multinuclear metal complexes.



Masayuki Nihei was born in 1974 in Tokyo. He received his B.S. (1997) from Keio University, and his M.S. (1999) and Ph.D. (2002) from the University of Tokyo. His Ph.D. work was devoted to the creation of photo- and proton-responsive azo-conjugated metalladithiolenes under the supervision of Prof. H. Nishihara. He joined Prof. H. Oshio's group at University of Tsukuba in 2002 as an assistant researcher and started to work on syntheses and their magnetic properties of multinuclear homo- and hetero-metal clusters. He became a research associate in December 2002 and an assistant professor in 2005 (Prof. H. Oshio's group at University of Tsukuba). His current research interests are concerning the development of versatile synthetic methods for multinuclear clusters and multi-functional systems with external stimuli response.